International Research Journal of Engineering and Technology (IRJET) e-ISSN: 2395-0056
Volume: 05 Issue: 03 | Mar-2018 www.irjet.net p-ISSN: 2395-0072

Controlling a Multi-Evaporator Refrigeration System That Uses Cuo/R134a Nano-Fluid

Khaled M. K. Pasha

Associate professor of mechanical power, Faculty of Engineering, Modern University, Mokatam, Cairo, Egypt

---

Abstract - *The present work is a trial to control more than one evaporator in a refrigeration system, which uses CuO/R134a Nano-Fluid as a refrigerant. To achieve this aim, two tasks were accomplished; the first is to investigate experimentally the variation of the 'evaporator ' heat transfer coefficient with the heat flux, Nano-Fluid mass flux, and Nano-Particles s mass concentration, z. This was implemented using a traditional vapor compression refrigeration system. For all studied cases, the heat transfer coefficient increased with the heat and mass fluxes and, for the same value of heat or mass fluxes the heat transfer coefficient increased with the Nano-Particles concentration up to 0.5 %, and beyond this value, it started to decrease again. The maximum enhancement in the heat transfer coefficient was about 110% and occurred when increasing the heat flux by about 100.9% of its lowest value. Two correlations were suggested to fit the data of the heat transfer, the Nano-Particles s concentration and the heat and mass fluxes. The second task is to modify the refrigeration system with an auxiliary evaporator and to use the experimental results from the first task to control the heat and mass fluxes, in order to control the heat transfer coefficient and accordingly, to achieve a predetermined variation of the cooling behavior. This trial could be taken as a step towards a future work, where, it is possible to control many evaporators using one compressor.*

Key Words: refrigeration, Nano-Fluid, heat transfer coefficient.

1. INTRODUCTION

1.1 Survey of Previous Works

Because of the widespread of the refrigeration and HVAC systems, that became an essential part of human life, many researchers have been investigating different techniques to enhance the heat transfer in the system components, especially in the evaporator. One of these techniques is the use of a Nano-Fluid that has the high thermal conductivity of the solids and the convective characteristics of the liquids. Different models were suggested to interpret the mechanism of heat enhancement when using a Nano-Fluid, but, none of them is approved. Mahesh Suresh Patil [1] et al reviewed many Nano-Fluid thermal behavior and concluded that, the highest rise in the COP of 15% in an Al2O3/R134a system occurred at higher temperatures because of the enhanced thermal conductivity, and a reduction of 11% in compressor work was observed when the TiO2 Nano-Particles s were suspended in mineral oil and used with a base refrigerant. Rupesh, et al, [2], performed experiments to analyze thermodynamically the minimum temperature difference (T) of a cascade condenser of cascade refrigeration system using R134a-R23 in order to get maximum COP of the system, by considering different operating parameters. The operating parameters include: (1) the condensing and evaporating temperature of R134a, (2) the condensing and evaporating temperature of R23. This analysis was also done on a cascade refrigeration system using R134a-R23 as refrigerant pairs. Both the experimental and the theoretical results were in good agreement with each other. T.M. Yusof, et al, [3], performed an experimental investigation of the performance of a domestic refrigerator working with POE-Al2O3 / R134a Nano-Fluid, with 0.2% volume concentration. The energy consumption in the domestic system was reduced by 2.1% at charging pressure of 42 psi. K. S. M.Naas, [4], investigated the heat transfer augmentation in a domestic refrigeration system for two Nano-Particles s; CuO and TiO2 with a volume concentration ranged from 0.05 to 1 %. He concluded that the evaporator heat transfer coefficient increases with the increase of both mass and heat fluxes, and that increase reached a value of 50% of the pure fluid case with CuO Nano-Particles s, and the heat transfer of a CuO/R134a is higher than that of TiO2/ R134a. Coumaressin, et al, [5], designed a successful model to simulate the heat transfer behavior of the refrigeration system, which uses CuO Nano-Particles with R134a refrigerant. The obtained results indicated an increase in the evaporating heat transfer coefficient with the usage of nano CuO. Fadhilah, et al, [6], investigated, the effect of the suspended copper oxide (CuO) Nano-Particles s into the 1, 1, 1, 2-tetrafluoroethane, R-134a by using mathematical modeling. The investigation includes the thermal conductivity, dynamic viscosity, and heat transfer rate of the Nano-Refrigerant in the tube of the evaporator. His results showed that, adding 1% vol. The fraction of nano-particles into the refrigerant has increased the thermal conductivity by about 312%. Sendil kumar, et al, [7], investigated ZnO Nano-Refrigerant in R152a refrigeration system and concluded that; maximum COP of 3.56 was obtained with 0.5% concentration of ZnO, and 21% of power reduction was obtained. Ahmad Reza Sajadi, et al, [8] investigated the heat transfer and pressure drop behavior of ZnO/water Nano-Fluid flow inside a circular tube with constant wall temperature, volume fractions of 1% and 2%, and the Reynolds numbers ranged from 5000 to 30000. Their results indicated that heat transfer coefficient increased by 11% and 18% when increasing

the volume fraction of Nano-Particles s to 1% and 2% vol, respectively, and the pressure drop was 45% and145%, respectively, higher than that of the base fluid. Mahbubul, et al, [9], investigated experimentally the heat transfer and pressure drop characteristics of Al_2O_3-R141b Nano-Refrigerants for different volume concentrations in vapor compression refrigeration system. Both heat transfer and pressure drop characteristics increased with the enhancement of Nano-Particles volume concentrations. Javadi, et al, [10], investigated the pattern of electricity generation for 39 years since 1991–2030 and the energy saving of a domestic refrigerator in Malaysia, and concluded that; the use of 0.1% TiO2–mineral oil–R134a Nano-Refrigerant has caused a maximum energy saving of (25%), and the effect of 0.06% TiO2 is more than that of 0.1% Al2O3. Subramani. N, et al, [11], performed experimental and theoretical studies to evaluate the performance parameters of a vapor compression system with pure SUNISO 3GS oil and with different Nano-Lubricants. Freezing capacity was higher for TiO2 Nano-Lubricant compared with other studied cases, and the power consumption of the compressor is reduced by 15.4%. Muhammad Abbas, et al, [12], added CNT Nano-Particles s into POE lubricant and mixed them with R-134a. They obtained COP value of 3.757 at 0.1% of CNT. Kumar, et al, [13], experimentally studied the performance parameters of a vapor compression refrigeration system with different Nano-Lubricants. Freezing capacity increased with the R600a refrigerant and with mineral oil + alumina Nano-Particles s oil mixture compared with the system which uses POE oil.The power consumption of the compressor decreased by 11.5% when the Nano-Lubricant is used instead of conventional POE oil. Venkataramana, et al, [14], used a Mineral oil (MO) with 0.1 g L^{-1} TiO2 Nano-Particles s mixture, as the lubricant *instead* of Polyol-ester (POE) oil in the R134a, R436A (R290/r600a-56/44-wt.%) and R436B (R290/r600a-52/48-wt.%),VCRSS. They found out that, VCRSS total irreversibility at different processes was better than the R134a, R436A and R436B and POE oil system. The same tests with Al_2O_3 Nano-Particles s showed that the different Nano-Particles s properties have little effect on the VCRS irreversibility. Kumar and Elansezhian, [15], performed an experimental investigation on the Nano Al2O3-PAG oil in R134a in a vapor compression refrigeration system. The results indicated that, when using lubricant with 0.2%V concentration of nano Al2O3, energy reduction of about 10.32% than that when using a pure lubricant. The Maximum COP of 3.5 is achieved for a capillary length of 10.5 m. Shengshan Bian, [16] et al, experimentally investigated the Nano-Refrigerant TiO2-R600a in a domestic refrigerator using energy consumption test and freeze capacity test. Their results indicated that, the refrigerator performance was better than the pure R600a system, with 9.6% less energy when the concentration is 0.5 g L^{-1} TiO2-R600a Nano-Refrigerant. Subramani and Prakash, [17], performed experimental studies to evaluate the performance parameters of a vapour compression refrigeration system with different lubricants including Nano-Lubricants. They concluded that, using R134a refrigerant and alumina Nano-Particles oil mixture, freezing capacity of the refrigeration system is increased compared to that when using POE oil. The power consumption of the compressor reduces by 25% when the Nano-Lubricant is used instead of conventional POE oil, and The coefficient of performance of the refrigeration system also increases by 33%. Peng et al, [18], investigated the influence of nanoparticles on the heat transfer characteristics of refrigerant-based nanofluid flow boiling inside a horizontal smooth tube, and presented a correlation for predicting heat transfer performance of refrigerant-based nanofluid. They used R113 refrigerant and CuO nanoparticles, and their experimental conditions included an evaporation pressure of 78.25 kPa, mass fluxes from 100 to 200 kg m2 s1, heat fluxes from 3.08 to 6.16 kW m2, inlet vapor qualities from 0.2 to 0.7, and mass fractions of nanoparticles from 0 to 0.5 wt%. they concluded that the heat transfer coefficient of refrigerant-based nanofluid is larger than that of pure refrigerant, and the maximum enhancement of heat transfer coefficient is 29.7%. Sundar and Singh, [19], reviewed the enhancement techniques of the heat transfer researches. They summarized the correlations developed for heat transfer coefficient and friction factor, and developed the correlations for the estimation of Nusselt number for different kinds of nano-fluids flowing in a plain tube under laminar and turbulent conditions.

1.2 Objectives of the Present Work

In the present work, it is intended to accomplish *"two tasks*"; *the first,* is to design and implement a refrigeration unit, Whose refrigerant is a Nano-Fluid, (CuO/R143a), with average Nano-Particles s size of about 40 nm, in order to investigate experimentally the variation of heat transfer coefficient of the evaporator with the heat and mass fluxes and the Nano-Particles concentration, (z). *The second* is to modify the system with an auxiliary evaporator and to supply the experimental data to a prepared control unit which can vary the heat and mass fluxes in order to achieve a predetermined heat transfer behavior. Table 1 illustrates the different studied cases.

Table 1 Cuo Mass Concentration, Mass Flux, and Heat Flux for the Investigated Cases

concentration of CuO %	Heat flux, q, (kW m^{-2})	Mass flux, G, ($kg.m^{-2}$ s^{-1})
0.05	33.63	125.5
0.05	44.73	166.8
0.05	56.4533	209.3
0.05	67.8	251.6
0.5	34	126
0.5	45.14	167.4
0.5	57.14	210.1

0.5	68.49	252.4
1	33.8	126.3
1	44.6	168
1	56.85	210.6
1	68	253

2. EXPERIMENTAL WORK

The first task of the present work is accomplished using a primary test rig, figure 1, and following are the details of its components;

2.1 The Primary Test Rig

The primary test rig consists mainly of two loops; one is for refrigerant and the other is for water. In the first loop, the refrigerant evaporates in the evaporator (4) and enters the compressor (1), where it is compressed to the condenser pressure, and is condensed by the water-cooled condenser (2). The liquid refrigerant flows through the adjustable throttle valve (3), Dofun-TVD-A, that is adjusted to maintain the evaporator and condenser pressures according to the compressor inlet and outlet pressures.

The refrigerant is throttled to the evaporator pressure. A flow meter (5) is placed after the condenser to measure the refrigerant flow rate. In the second loop, the water is circulated from the pump, (7) at a fixed rate of 0.74 kg/s to the evaporator, where, it flows around the refrigerant tube in opposite direction to that of the refrigerant. This *relatively warm* water represents the thermal load which will evaporate the refrigerant. The *cooled* water leaves the evaporator to the condenser to condense the refrigerant, then, it is delivered to the drain. The arrangement of the test rig is similar to that, which is mentioned in [5], and it will be described in the following paragraphs;

2.1.1the Compressor, (1)

The compressor is of type TECUMSEH sealed hermetic reciprocating type of one HP, 220 volts, and 50 Hz.

2.1.2 The Condenser, (2)

The condenser is a heat exchanger, which consists of two concentric copper tubes, and has a length of 1700 mm. The inner tube, where the refrigerant flows, has an outer diameter of 9.52 mm,(3/8 inch), and the inner diameter of 7.72 mm, (2.47/8 inch). The outer tube, where the water flows, has an outer diameter of 19.05 mm,(3/4 inch), and the inner diameter of 17 mm, (0.68 inches).

2.1.3 The Main Evaporator, (4)

The main evaporator is a heat exchanger which consists of two concentric copper tubes and has a length of 1260 mm.

The inner tube, where the refrigerant flows, has an outer diameter of 9.52 mm,(3/8 inch), and an inner diameter of 7.72 mm, (2.47/8 inch). The outer tube, where the water flows, has an outer diameter of 19.05 mm, and the inner diameter of 17.25 mm. The outer tube is divided into 10 segments, each segment has an independent inlet and exit terminals as shown in figure 2. This structure promotes for the turbulent mixing activities of the flowing water and accordingly, enhances the evaporation of the flowing refrigerant.

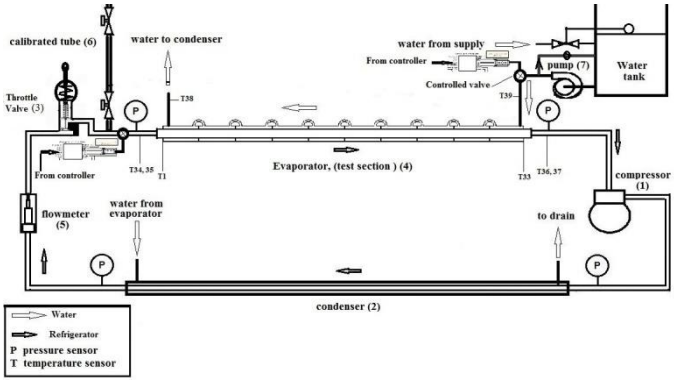

FIGURE 1 THE PRIMARY TEST RIG

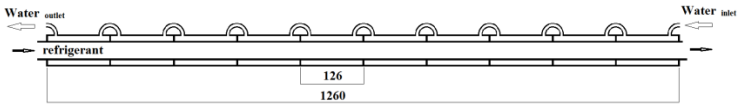

FIGURE 2 THE MAIN EVAPORATOR

2.1.4 The Pump

The water pump is QB Series Peripheral 0.25 hp water pump, which is interfaced to the controller which controls the water discharge.

2.1.5 Measuring and Control Devices

The following devices are connected to PIC32MX3/4 microcontroller; the calibrated thermocouples of type (T), which are distributed as follows; thirty-three thermocouples, T1 to T33, are distributed on eleven positions on the surface, another two pairs of thermocouples, T34 to T37, are placed in the refrigerant flow passage, before and after the evaporator.

To measure the change in water temperature, two thermocouples, T38 and T39, are placed in the *water* passage before and after the evaporator. These thermocouples are connected to the controller by three TCA9546-i2C Mux and six i2c-MCP9600 thermocouple chips. Four pressure sensors are distributed as follows; two of them are placed before and after the evaporator, and each of them has a maximum reading of 10 bars, and the other two sensors are placed before and after the condenser, each of them has a maximum reading

of 32 bars. Two control valves that are controlled by stepper motors with their drivers. Each valve is first calibrated to determine the relation between the motor turns and the corresponding flow rate. Then, they are installed in the passages of the water and refrigerant before the evaporator. The refrigerant flow rate is measured using an Omega F1-2100A flow meter, (5), which measures values from 0.2 to 1.9 liter min^{-1}, with accuracy 0.05 liter.min^{1}. The high and low cycle pressures are adjusted using an adjustable throttle valve (3), Dofun-TVD-A. The water flow rate is measured using a DZ-4002 flow meter, which measures values from 1.8 to 18 liter min^{-1}. The masses are weighed by an electronic balance RUIM D-8001 with Readability 0.01 gm. The signals from thermocouples, pressure sensors, and the flow rate sensors are fed from the microcontroller to a PC, which calculates the corresponding heat flux, mass flux and heat transfer coefficient, equations 8, 10 and 11.

2.2 The Experimental Procedure

Before beginning, the following procedure is followed;

- operating the pump at max power for 10 minutes to check the water passages
- The fabricated experimental setup is filled with N2 gas at a pressure of 7 bar and this pressure is maintained for 45 minutes for the purpose of leakages check, (5).
- reviewing the connections between the control components and measuring devices
- The cycle is evacuated using a vacuum sealed vessel.

In every experiment, the following steps were followed;

1) weighing the calculated mass of Nano-Particles s, using digital electronic balance, and adding them carefully to the corresponding weight of Emcarate RL 32 POE oil, according to table 2.
2) The mixture is placed on the ultrasonic vibrator for 3 hours to ensure uniform dispersion of Nano-Particles s, [5].
3) The mixture is further kept vibrating for an additional half an hour, on an ultrasonic homogenizer to fully separate the Nano-Particles and to prevent any clustering of particles in the mixture, and to obtain proper homogenization, and then added to the cycle.
4) Operating the compressor and after 10 minutes, the controller starts to feed the computer with the signals of temperature before and after the evaporator for the water and refrigerant, and the signals from the flow meters of both liquids. The program calculates the corresponding average surface and refrigerant temperatures, equation (1-3). It then uses equations (4-8) and 11, beside formulas that fit the relations between the thermodynamic properties of both the particles and the base fluid, in order to calculate the different Nano-Fluid properties and an *initial* value for the water flow rate.
5) The controller adjusts the water valve opening according to this value. Keeping receiving newer signals from these sensors, the program *recalculates newer* water flow rates, and according to a PID technique, the water rate keeps modifying until the difference between the newer and older values is within 2%.
6) After achieving the steady state, the program uses the input data to calculate the corresponding heat transfer coefficient.

Table 2 Preparing the Nano-Lubricant

Nano-Particles concentration, z	Z = 0.05 %	Z = 0. 5 %	Z = 1 %
Lubricant, (gram)	3	30	60
R134a, (gram)	596.7	567	534
Nano, (gram)	0.3	3	6

According to [4];

$$T_{s,av} = \frac{\sum_{1}^{33} T_{si}}{33} \quad (1)$$

$$T_{si} = (T_{top}\, T_{side}\, T_{bottom})_i \quad (2)$$

$$T_{nf,av} = (T_{in} + T_{out})_{nf}/2 \quad (3)$$

$$100\,\phi = \frac{z\rho_f}{\rho_{np}(1-z)+z\rho_f}, \qquad \rho_{nf} = \phi\rho_{np} + (1-\phi)\rho_f \quad (4)$$

(5)

$$Cp_{nf} = \frac{\phi(\rho Cp)_{np} + (1-\phi)(\rho Cp)_f}{\rho_{nf}} \quad (6)$$

$$\mu_{nf} = \mu_f (1-\phi)^{2.5} \quad (7)$$

$$\overset{*}{m} = (\overset{*}{V}\rho)_{nf} \quad (8)$$

$$Re = \frac{4\overset{*}{m}_{nf}}{10^3 \pi d_i L\ \mu_f} \quad (9)$$

The program estimates an *initial water* flow rate, $\overset{*}{m}_w$ from an intended heat flux $\overset{*}{q}$, according to;

$$\overset{*}{q} A_s = \overset{*}{m}_w C_w (T_{iw} - T_{ow}) \quad (10)$$

$$h = \frac{[\overset{*}{m}\, Cp(T_o - T_i)]_{nf}}{\pi d_i L(T_{s,av} - T_{nf,av})} \quad (11)$$

The cycle coefficient of performance;

$$C.O.P = \frac{Cp(T_o - T_i)]_{nf,e}}{Cp(T_o - T_i)]_{nf,c}} \quad (12)$$

The worst *relative* errors that may occur when measuring the above quantities are illustrated in Appendix A. To validate the experimental results, the data were compared to the previous work of both Naas, [4] and Peng et al, [18]. The comparison is performed for the variation of heat transfer coefficient with both the heat and mass fluxes, with Nano-Particles concentration of 0.5 %. Figures 3 and 4 illustrate comparisons of the present work with both [4] and [18], in which, the heat transfer variation, with both the heat and mass fluxes, are compared for a Nano-Particles concentration by mass, z = 0.5. It is obvious in figure 4 that, the results of the present work, are more close to those of [18]. That is because the method of measuring the heat flux is similar to that of [18], who used the saturation conditions to calculate the heat flux in the evaporator. In figure 5, the results of the present work, are more close to those of [4],

that may be because, the procedure of determining the mass flux is similar to that of [4], who used the average evaporator conditions to calculate the Nano-Fluid density and accordingly, the mass flux.

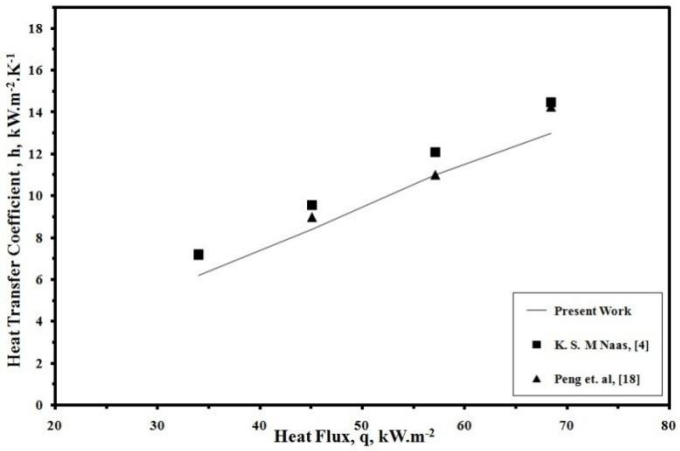

FIGURE 3 VARIATION OF THE HEAT TRANSFER COEFFICIENT WITH THE HEAT FLUX FOR THE PRESENT WORK AND BOTH; [4], AND [18].

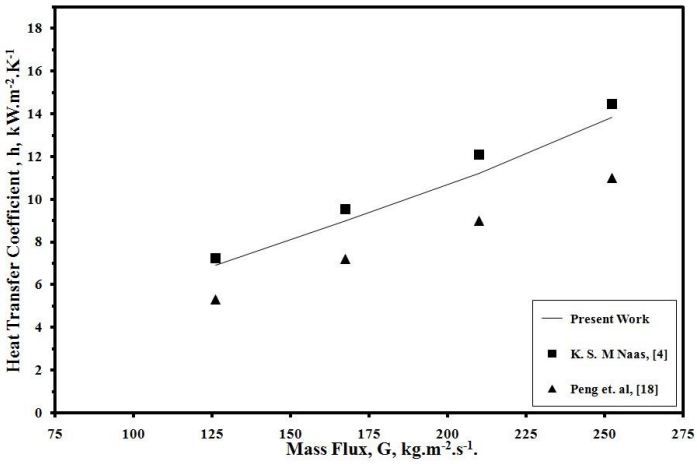

FIGURE 4 VARIATION OF THE HEAT TRANSFER COEFFICIENT WITH THE MASS FLUX FOR THE PRESENT WORK AND BOTH [4] AND [18].

3 RESULTS AND DISCUSSION

3.1 Experiments of the First Task

These experiments are executed to investigate the variation of the heat transfer coefficient, with the heat and mass fluxes and the particles concentration. Figure 5 illustrates the variation of the heat transfer coefficient with the heat flux and Figure 6 illustrates the variation of the heat transfer coefficient with the mass flux. First observation in the two figures is that the position of each data point of the heat and mass fluxes differs slightly with the increase of particles concentration. That is because, as mentioned before the controller estimates an initial value for the water flow rate and try to modify it according to the intended heat flux until fluctuating about the intended value with 2% fluctuations about this value, and then start to calculate the corresponding heat transfer coefficient. And increasing the concentration leads to an increase in the mass flow rate and accordingly, the Reynolds number. Also, the increase in the particles concentration with its higher thermal conductivity improves the mixture thermal conductivity, which affects the heat flux. All these factors affect the controller accuracy when trying to reproduce the same values of heat and mass fluxes for different particle concentrations. Another observation is that, for all studied cases, the heat transfer coefficient increases with the particles concentration until z =5% and beyond this value, it start to decrease again. That may be because, when the particles concentration increases, the mass flow rate increases too, equation 4 and 8, and accordingly the heat transfer rate increases, and the possibility of increasing the bulk fluid temperature increases too. So, the difference between the fluid and the surface decreases, which helps the increase of the heat transfer coefficient, equation 11.

But, increasing the particles concentration may lead to a reduction in the Nano-Particles Brownian motion and the motion due to the action of thermophoretic forces and accordingly, its convective heat transfer may decrease. So, increasing the Nano-Particle concentration produces two opposing factors; one promotes for the increase in heat transfer coefficient, which is dominant for a concentration less than 0.5 %, and the other factor decays the heat transfer and is dominant for a concentration greater than 0.5 %. In figure 4, the heat transfer coefficient increases with the heat flux, for all values of concentration. That may be because, increasing the heat flux, promotes for a higher refrigerant superheat, which in turn increases the average refrigerant temperature and reduces the temperature difference between the refrigerant and the surface. This leads to an increase in heat transfer coefficient. In figure 5, the heat transfer coefficient increases with the mass flux, for all values of concentration. That may be because, increasing the fluid flow rate promotes for a higher possibility of exchanging more thermal energy with the tube surface, which leads to a decrease in the average temperature difference between the surface and fluid, so the ratio between heat flux and the temperature difference increases, and accordingly, the heat transfer coefficient.

The maximum percentage of enhancement in the heat transfer coefficient was 110 %, which occurred when increasing the heat flux by about100.9 % of its lowest value. Figure 7 illustrates the variation of C.O.P with the heat transfer coefficient. For all Nano-Particle concentration, the C.O.P varies slightly with the heat transfer coefficient, which reflects that the heat transfer increases at a greater rate than that of the compressor power. That may be because the compressor power and the cycle losses are almost proportional to the refrigerant mass flow rate. But the relation between the heat transfer rate and the refrigerant mass flow rate is not linear. For the same heat transfer coefficient, the COP increased with the particle concentration until the value of 0.5%, and beyond this value, it starts to decrease again. This may be because the concentration slightly affects the compressor power, unlike the heat transfer coefficient, which is affected by the concentration as mentioned above. The following two correlations were suggested to fit the experimental results of the heat transfer coefficient, Nano-Particles concentration, the heat flux and the mass flux;

for 0.05% < z < = 0.5%;

$$h = 1.696 * z^{0.056} * q^{2.75} * G^{-1.73} \quad (13)$$

for 0.5% < z < = 1.0%;

$$h = 0.05 * z^{-0.097} * q^{0.13} * G^{0.91}, \quad (14)$$

Appendix (B) illustrates the tests of the two correlations. The tests indicated that the worst percentage of the difference between the calculated and measured heat transfer coefficient was about 3%.

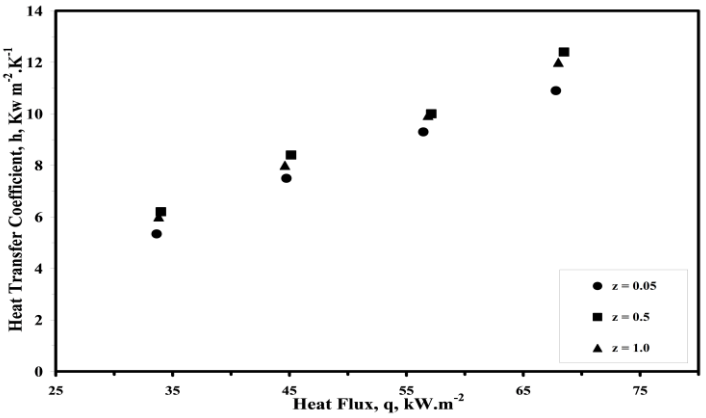

Figures 5 Variation of the Heat Transfer Coefficient with Heat Flux

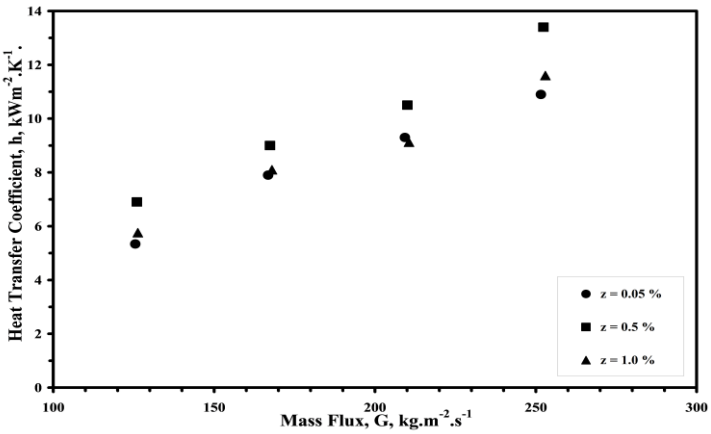

Figures 6 Variation of the Heat Transfer with Mass Flux

Figures 7 illustrates the variation of COP with heat transfer coefficient. The COP varies slightly with (h), which reflects that operating the Nano-refrigerant system at higher heat transfer performance is accompanied by a *little* reduction in the power cost per unit of refrigeration load.

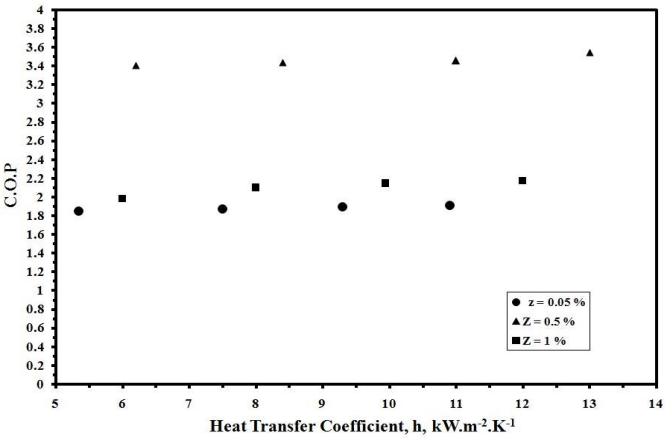

Figure 7 Variation of the Coefficient of Performance with the Heat Transfer Coefficient.

3.2 Controlling the Heat Transfer Coefficient

In these experiments, it is required to vary the heat transfer coefficient of the main evaporator with time according to a predetermined behavior. Figure 8 illustrates the preparation of the control experiment. The figure illustrates a secondary evaporator, which is similar to the main evaporator and is installed to share the water and refrigerant flow rates with the main evaporator. The two controlled valves are installed in the entrance to the main evaporator; one of them controls the refrigerant flow rate and the other controls the hot water flow rate. The experimental data of the heat and mass fluxes, and the heat transfer coefficient, that is extracted from the experiments, whose Nano-Particles concentration is 0.5 % are fed to the program. According to these data, the controller produces the required variation in the heat and mass fluxes and accordingly, the required heat transfer coefficient. To execute this type of experiments, the preparations and steps from (1 to 5) that are mentioned in 2.2 are followed. First, the program should adjust the system devices to produce a heat flux of 33.5 $kW.m^{-2}$ and a mass flux of 124 $kg.s^{-1}.m^{-2}$ which correspond to a heat transfer coefficient of about 6 $kW.m^{-2}K$.

(1) Then the heat transfer coefficient should be maintained at the value of 6 $kW.m^{-2}.k^{-1}$ for 40 minutes.

(2) Next, the heat transfer coefficient should be maintained at a value of 12 $kW.m^{-2}.K^{-1}$ for 120 minutes. This value corresponds to a heat flux of 62.5 $kW.m^{-2}$ and a mass flux of 231 $kg.s^{-1}.m^{-2}$

(3) Next, the heat transfer coefficient should be maintained at a value of 10 $kW.m^{-2}.K^{-1}$ for 60 minutes. This value corresponds to a heat flux of 53.2 $kW.m^{-2}$ and a mass flux of 196.1 $kg.s^{-1}.m^{-2}$

The variation of the heat transfer coefficient with both the heat and mass fluxes are monitored every 10 minutes.

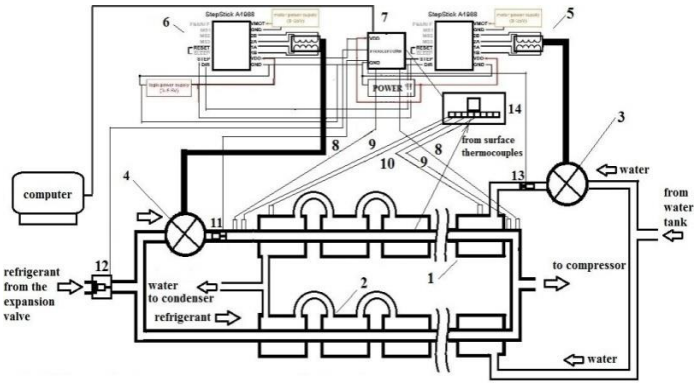

Figure 8 The Control Unit Installation.

In the beginning of each interval, the controller changes the mass and heat fluxes according to the values that are mentioned above, and a PID scheme helps these quantities to approach the required values with 2% fluctuation about each one. Consequently, the corresponding heat transfer coefficient is approached. This scheme keeps guarding the achieved values to maintain them from the random change in the ambient conditions and unpredicted losses. Figure 9 illustrates the variation of heat transfer coefficient with time.

It is observed that the heat transfer coefficient value during each of the three intervals is not stable, that is because of the limited speed and storage capacity of the used controller which did not ensure the proper speed of response to the feedback signals. That is beside the fluctuating nature of the variation in the ambient conditions during the day hours, which is an inherent characteristic of the weather in the city, where these experiments are performed. These random variations may lead to unpredicted losses in the hot water side as well as the refrigerant side of the refrigeration system.

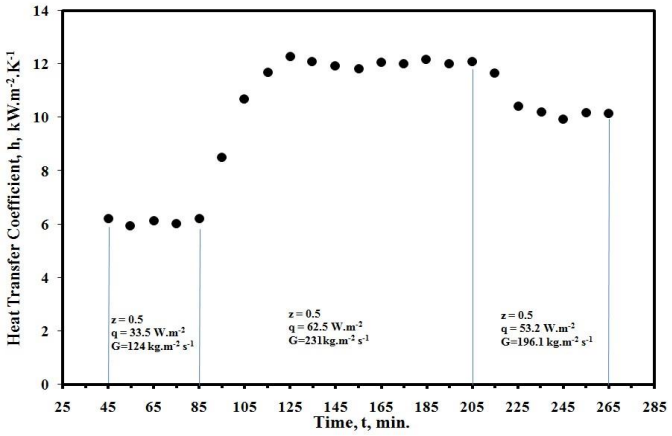

Figure 9 The Controlled Heat Transfer Coefficient

4. CONCLUSION

The *first* task of the present work is to investigate experimentally the variation of the *'evaporator '* heat transfer coefficient with the heat flux, mass flux, and Nano-Particles concentration in a vapor compression refrigeration system, whose refrigerant is a CuO/R134a Nano-Fluid. The heat transfer coefficient increased with the heat and mass fluxes and, for the same value of heat or mass fluxes, the heat transfer coefficient increased with the Nano-Particles concentration up to 0.5 %, and beyond this value, it started to decrease again. The maximum percentage of enhancement in the heat transfer coefficient was 110 %, which occurred when increasing the heat flux by about100.9 %. Correlations were suggested to fit the data of the heat transfer coefficient, mass and heat fluxes and the Nano-Particles mass concentration. The *second* is to modify the refrigeration system to be capable of controlling the heat and mass fluxes in order to achieve a

predetermined cooling behavior. The heat transfer from the evaporator could be controlled to an acceptable extent by the designed control unit.

REFERENCES

[1] Mahesh Suresh Patil, Sung Chul Kim, Jae-Hyeong Seo, and Moo-Yeon Lee, "Review of the Thermo-Physical Properties and Performance Characteristics of a Refrigeration System Using Refrigerant-Based Nanofluids", Published: 31 December (2015), MDPI, journal of Energies, 2016, 9, 22; doi:10.3390/en9010022www

[2] P. L. Rupesh, J. M. Babu, D. Surryaprakash, and R. D. Misra, "Experimental and computational evaluation of temperature difference of a cascade condenser of R134a-R23 cascade refrigeration system", International Conference on Smart Technologies and Management for Computing, Communication, Controls, Energy and Materials (ICSTM), (2015) Chennai, 6-8 May (2015), Page(s): 659 - 663

[3] T.M. Yusof, A.M. Arshad, M.D. Suziyana, L.G. Chui, and M.F. Basrawi "EXPERIMENTAL STUDY OF A Domestic Refrigerator With Poe-Al2o3 Nanolubricant", International Journal Of Automotive And Mechanical Engineering, Issn: 2180-1606 (Online); Volume 11, Pp. 2243-2252, January-June (2015)

[4] K. S. M.Naas,"Heat Transfer Enhancement in Vapor Compression Refrigeration System Using Nano-Fluidwith R-134a", Thesis, Benha University, Faculty Of Engineering, Mechanical Engineering Department, (2015).

[5] T. Coumaressin and K. Palaniradja, "Performance Analysis of a Refrigeration System Using Nano Fluid ", International Journal of Advanced Mechanical Engineering, ISSN
2250-3234 Volume 4, Number 4 (2014), pp. 459-470

[6] S. A. Fadhilah, R. S. Marhamah, anda.H.M.Izzat, "Copper Oxide Nanoparticles for advanced Refrigerant Thermophysical Properties: Mathematical Modeling", Journal of Nanoparticles, Volume (2014), Article ID 890751, 5 pages

[7] D. Sendil Kumar, R. Elansezhian, " ZnO nano-refrigerant in R152a refrigeration system for energy conservation and green environment", Front. Mech. Eng. (2014), 9(1): 75–80, DOI 10.1007/s11465-014-0285-y.

[8]Ahmad Reza Sajadi, Seyed Soheil Sadati, Masoud Nourimotlagh, Omid Pakbaz, Dariush Ashtiani, And Farshad Kowsari, "Experimental Study On Turbulent Convective Heat Transfer, Pressure Drop, And Thermal Performance Characterization Of ZnO/Water NanofluidFlow In A Circular Tube, Thermal Science (2014) Volume 18, Issue 4, Pages: 1315-1326 doi:10.2298/TSCI131114022S.

[9] I.M. Mahbubul, R. Saidur and M.A. Amalina, " Heat Transfer and Pressure Drop Characteristics of Al_2O_3-R141b Nano-refrigerant in Horizontal Smooth Circular Tube ", Procedia Engineering, Volume 56, (2013), Pages 323-329, 5th BSME International Conference on Thermal Engineering

[10] F.S. Javadi and R. Saidur, " Energetic, economic and environmental impacts of using nano-refrigerant in domestic refrigerators in Malaysia", Energy Conversion and Management Volume 73, September (2013), Pages 335–339

[11] Subramani.N, Aswin Mohan, and Dr.Jose Prakash.M, "Performance Studies On A Vapor Compression Refrigeration System Using Nano-Lubricant", international Journal of Innovative Research in Science, Engineering and Technology, Volume 2, Special Issue 1, December (2013), Proceedings of International Conference on Energy and Environment-On 12th to 14th December.

[12] Muhammad Abbas, Rashmi G. Walvekar and Farhood S.Javadi, "Efficient Air-Condition Unit By Using Nano-Refrigerant ", EURECA, (2013), pp 87 - 88.

[13] R. Reji Kumar,K. Sridhar, and M.Narasimha, "Heat transfer enhancement in domestic refrigerator using R600a/mineral oil/nano-Al2O3 as working fluid", International Journal of Computational Engineering Research||Vol, 03||(2013) ||page 42

[14] Venkataramana Murthy V. Padmanabhan, Senthilkumar Palanisamy, " The use of TiO2 nanoparticles to reduce refrigerator irreversibility", Energy Conversion and Management, Volume 59, July (2012), Pages 122–132

[15] D. Sendil Kumar and Dr. R. Elansezhian " Experimental Study on Al2O3-R134a Nano Refrigerant in Refrigeration System", International Journal of Modern Engineering Research (IJMER), Vol. 2, Issue. 5, Sep.-Oct. (2012) pp-3927-3929

[16] Shengshan Bi, Kai Guo, Zhigang Liu, Jiangtao Wu, Performance of a domestic refrigerator using TiO2-R600a nano-refrigerant as working fluid, Energy Conversion and Management, Volume 52, Issue 1, January (2011), Pages 733–737

[17] N. Subramani and M. J. Prakash, " Experimental studies on a vapor compression system using nano-refrigerants", International Journal of Engineering, Science and Technology, Vol. 3, No. 9, (2011), pp. 95-102

[18] Peng H., Ding G., Haitao, " heat transfer characteristics of refrigerant-based Nano-Fluid flow boiling inside a horizontal smooth tube", international journal of refrigeration, vol. 32, pp. 1259-1270.

[19], L. Syam Sundar, Manoj K. Singh "Convective heat transfer and friction factor correlations of nanofluid in a tube and with inserts: A review", Renewable and Sustainable Energy Reviews, 2013, vol 20, pp 23-35

ACKNOWLEDGMENT

I 'd like to thank prof. Mohammad Elfawal, mechanical department, the Modern University in Egypt for his sincere help in producing the present work. Thanks also are attended to all technicians and supervisors of the heat transfer lap. In the faculty of engineering, Modern University, Egypt for their kind help.

NOMENCLATURE AND ABBREVIATIONS

Alphabetic

A	area,	m^2.
C	specific heat,	$W.kg^{-1}.K^{-1}$
Cp	constant pressure specific heat,	$W.kg^{-1}.K^{-1}$
d	test section diameter,	m.
G	mass flux, $\dot{m}$ /cross section area,	$kg.s^{-1}.m^{-2}$
h	heat transfer coefficient,	$W.m^{-2}.K^{-1}$
L	test section length,	m.
m	mass	kg.
$\dot{m}$	mass flow rate,	$kg.s^{-1}$
p	pressure,	Pascal.
q^*	heat flux	$W.m^{-2}$.
T	temperature,	Kelven.
$\dot{V}$	volume flow rate	$m^3.s^{-1}$.
z	mass fraction,	%.

Subscript

av	average.
c	condenser.
e	evaporator.
f	Base fluid, (R134a + oil).
i	inlet.
nf	nano-fluid, refrigerant.
np	Nano-Particles s.
o	outlet.
s	evaporator surface
w	water

Greek Symbols

- The uncertainty in volume fraction.
- volume fraction.
- The uncertainty in heat transfer coefficient.
- dynamic viscosity.
- Density z
- The uncertainty in weight fraction.

Abbreviations

C O P	Coefficient of Performance
CuO	Copper Oxide
PID	Proportional, Integral, Derivative
POE	Polyester Oil
Ti O_2	Titanium Dioxide

Figure Captions List

Fig.1 The Primary Test Rig

Fig.2 The Main Evaporator

Fig.3 Variation Of Heat Transfer Coefficient With The Heat Flux For The Present Work And Both; [4], And [18].

Fig. 4 Variation Of Heat Transfer Coefficient With The Mass Flux For The Present Work And Both [4] And [18].

Fig.5 Variation Of The Heat Transfer Coefficient With The Heat Flux

Fig. 6 Variation Of The Heat Transfer Coefficient With The Mass Flux

Fig. 7 Variation Of The Coefficient Of Performance With The Heat Transfer Coefficient.

Fig. 8 The Control Unit Installation With Heat Transfer Coefficient.

Fig. 9 The Controlled Heat Transfer Coefficient

APPENDIXES

Appendix A: Error Analysis
To estimate the uncertainties of the *derived* quantities, z, and h, etc., we first recall the uncertainties of the *participating* quantities, which are;

Length is measured using a vernier caliper with uncertainty $\pm$ 0.02 mm

Temperature: the resolution of the digital indicator is $\pm$ 0.1 ^{o}C.

The Nano-refrigerant *volume* flow rate, $\dot{V}$, is measured with uncertainty of 0.05 $L.min^{-1}$

Mass is weighed with the readability of 0.01 gm.

Then, we can estimate the uncertainties in the derived quantities as follows;

$$\delta z = \left(\frac{m_{np}}{m_{np}+m_f}\right)\sqrt{\left(\frac{\delta m_{np}}{m_{np}}\right)^2+\left(\frac{\delta m_{np}^{\,2}+\delta m_f^{\,2}}{(m_{np}+m_f)^2}\right)} \qquad (A.1)$$

$$\delta\rho_{np} = \frac{z\,\rho_f}{\rho_{np}(1-z)+z\rho_f}\sqrt{\left(\frac{\rho_f\,\delta z}{\rho_f\, z}\right)^2+\frac{(\rho_{np}\,\delta z)^2+(\rho_f\,\delta z)^2}{(\rho_{np}(1-z)+z\rho_f)^2}}$$

(A.2)

$$\delta\rho_{nf} = \sqrt{(\delta\phi\,\rho_{np})^2+(\delta\phi\,\rho_f)^2}$$

(A.3)

$$\delta\dot{m} = (\dot{V}\,\rho_{nf})\sqrt{\left(\frac{\delta\dot{V}}{\dot{V}}\right)^2+\left(\frac{\delta\rho_{nf}}{\rho_{nf}}\right)^2}$$

(A.4)

$$\delta Cp_{nf} = \frac{\phi\rho_{np}\,Cp_{np}+(1-\phi)\rho_f\,Cp_f}{\rho_{nf}}\sqrt{\frac{(\rho_{np}\,Cp_{np}\,\delta\phi)^2+(\rho_f\,Cp_f\,\delta\phi)^2}{(\phi\rho_{np}\,Cp_{np}+(1-\phi)\rho_f\,Cp_f)^2}+\left(\frac{\delta\rho_{nf}}{\rho_{nf}}\right)^2}$$

(A.5)

$$\delta h = \frac{[\dot{m}\,Cp(T_o-T_i)]_{nf}}{\pi d_i L(T_{s,av}-T_{nf,av})}\sqrt{\left(\frac{\delta\dot{m}}{\dot{m}}\right)^2+\left(\frac{\delta Cp}{Cp}\right)^2+\left(\frac{\delta T^2+\delta T^2}{(T_O-T_i)^2}\right)^2+\left(\frac{\delta d_i}{d_i}\right)^2+\left(\frac{\delta L}{L}\right)^2+\left(\frac{\delta T^2+\delta T^2}{(T_{s,av}-T_{f,avi})^2}\right)^2}$$

(A.6)

$$\delta(C.O.P) = \frac{[Cp(T_o-T_i)]_{nf,e}}{[Cp(T_o-T_i)]_{nf,c}}\left[\left(\frac{2\delta Cp}{Cp}\right)_e^2+\frac{4\delta T^2}{(T_O-T_i)^2_c}\right]$$

(A.7)

According to the above formulas, the worst relative errors in the measured quantities are;

Relative error in measuring the weight ratio = 0.0017.

Relative error in measuring the volume fraction = 0.0016.

Relative error in measuring the nano-fluid density = 1.6 e-005.

Relative error in measuring the mass flow rate = 0.027.

Relative error in measuring the nano-fluid specific heat = 2.01 e-005.

Relative error in measuring the heat flux = 0.025.

Relative error in measuring the heat transfer coefficient = 0.0123819.

Relative error in measuring the COP = 0.0273.

Appendix B: Correlation Tests

Equation 13

EQUATION COEFFICIENTS

1.69581 0.0559713 2.75173 -1.72744

CALCULATED	MEASURED	Deviation %
5.40022	5.34	1.1
7.24176	7.5	3.1
9.28407	9.3	0.17
11.182	10.9	2.5
6.28747	6.2	0.01
8.3951	8.4	0.058
10.8467	11	1
13.0079	13	0.06

Equation 14

EQUATION COEFFICIENTS

0.046465 -0.0969923 0.125145 0.910458

CALCULATED	MEASURED	Deviation %
6.31362	6.2	1.8
8.47264	8.4	0.8
10.7316	11	2
12.9731	13	0.2
5.91154	6	1.4
7.93563	8	0.8
10.0492	9.94	1
12.1449	12	1.2